

1

2 A simple microbiome in the European common cuttlefish, *Sepia officinalis*

3

4 Holly L. Lutz^{a,b,c,†,*}, S. Tabita Ramírez-Puebla^{d,†}, Lisa Abbo^d, Amber Durand^d, Cathleen
5 Schlundt^d, Neil Gottel^{a,b}, Alexandra K. Sjaarda^e, Roger T. Hanlon^d, Jack A. Gilbert^{a,b,c}, Jessica
6 L. Mark Welch^{d,*}

7

8 ^aDepartment of Pediatrics, University of California San Diego, La Jolla, California, USA.

9 ^bScripps Institution for Oceanography, UCSD, La Jolla, California, USA

10 ^cIntegrative Research Center, Field Museum of Natural History, Chicago, Illinois, USA

11 ^dMarine Biological Laboratory, Woods Hole, MA 02543

12 ^eBiological Sciences Division, University of Chicago, Chicago, IL 60637

13

14

15

16 [†] co-first authors, contributed equally to this work

17 *to whom correspondence should be addressed. Email address: hlutz@fieldmuseum.org or

18 jmarkwelch@mbl.edu

19

20

21

22 ABSTRACT

23

24 The European common cuttlefish, *Sepia officinalis*, is used extensively in biological and
25 biomedical research yet its microbiome remains poorly characterized. We analyzed the
26 microbiota of the digestive tract, gills, and skin in mariculture-raised *S. officinalis* using a
27 combination of 16S rRNA amplicon sequencing, qPCR and fluorescence spectral
28 imaging. Sequencing revealed a highly simplified microbiota consisting largely of two
29 single bacterial amplicon sequence variants (ASVs) of Vibrionaceae and Piscirickettsiaceae. The
30 esophagus was dominated by a single ASV of the genus *Vibrio*. Imaging revealed bacteria in the
31 family Vibrionaceae distributed in a discrete layer that lines the esophagus. This *Vibrio* was also
32 the primary ASV found in the microbiota of the stomach, cecum, and intestine, but occurred at
33 lower abundance as determined by qPCR and was found only scattered in the lumen rather than
34 in a discrete layer via imaging analysis. Treatment of animals with the commonly-used antibiotic
35 enrofloxacin led to a nearly 80% reduction of the dominant *Vibrio* ASV in the esophagus but did
36 not significantly alter the relative abundance of bacteria overall between treated versus control
37 animals. Data from the gills was dominated by a single ASV in the family Piscirickettsiaceae,
38 which imaging visualized as small clusters of cells. We conclude that bacteria belonging to the
39 Gammaproteobacteria are the major symbionts of the cuttlefish *Sepia officinalis* cultured from
40 eggs in captivity, and that the esophagus and gills are major colonization sites.

41

42

43 IMPORTANCE

44

45 Microbes can play critical roles in the physiology of their animal hosts, as evidenced in
46 cephalopods by the role of *Vibrio (Aliivibrio) fischeri* in the light organ of the bobtail squid and

47 the role of Alpha- and Gammaproteobacteria in the reproductive system and egg defense in a
48 variety of cephalopods. We sampled the cuttlefish microbiome throughout the digestive tract,
49 gills, and skin and found dense colonization of an unexpected site, the esophagus, by a microbe
50 of the genus *Vibrio*, as well as colonization of gills by Piscirickettsiaceae. This finding expands
51 the range of organisms and body sites known to be associated with *Vibrio* and is of potential
52 significance for understanding host-symbiont associations as well as for understanding and
53 maintaining the health of cephalopods in mariculture.

54

55 KEYWORDS:

56 microbiome, fluorescence *in situ* hybridization, Cephalopoda, Vibrionaceae, Piscirickettsiaceae,
57 enrofloxacin

58

59 1. INTRODUCTION

60

61 Symbiotic associations between invertebrates and bacteria are common. Among cephalopods, the
62 most intensely studied association is the colonization of the light organ of the bobtail squid
63 *Euprymna scolopes* by the bioluminescent bacterium *Vibrio (Aliivibrio) fischeri* in a highly
64 specific symbiosis (1). A more diverse but still characteristic set of bacteria colonize the
65 accessory nidamental gland from which they are secreted into the egg jelly coat and likely
66 protect the eggs from fungal and bacterial attack (2). The accessory nidamental gland and egg
67 cases of the squid *Doryteuthis (Loligo) pealeii* and the Chilean octopus (*Octopus mimus*) have
68 also been reported to contain Alphaproteobacteria and Gammaproteobacteria (3, 4). These
69 associations indicate that bacteria can play a key role in the physiology of cephalopods.

70 *Sepia officinalis*, the European common cuttlefish (hereafter cuttlefish), is used
71 extensively in biological and biomedical research (5-7) and is a model organism for the study of
72 rapid adaptive camouflage (8-11). Cuttlefish are also widely represented among zoos and
73 aquaria, and play an important role in educating the public about cephalopod biology and life
74 history (12). Little is known about the association of bacterial symbionts with cuttlefish, and
75 whether such associations may play a role in the health or behavior of these animals.
76 Understanding the importance, or lack thereof, of the cuttlefish microbiome will not only shed
77 light on the basic biology of this model organism but will also have important implications for
78 future husbandry practices and research design.

79 Using a combination of 16S rRNA amplicon sequencing, fluorescence *in situ*
80 hybridization (FISH), and quantitative PCR (qPCR), we characterized the gastrointestinal tract
81 (GI), gill, skin, and fecal microbiota of the common cuttlefish in wild-bred, captive-raised
82 animals (5) housed at the Marine Biological Laboratory (Woods Hole, MA). We observed a
83 highly simplified microbiome dominated by Vibrionaceae in the gastrointestinal tract and
84 Piscirickettsiaceae in the gills. We treated a subset of cuttlefish with antibiotic enrofloxacin,
85 commonly used among aquaria veterinarians, and found both ASVs to remain dominant in
86 esophagus and gill microbiota, suggesting they are resilient to this antibiotic. The simplicity of
87 this system makes it a promising model for further exploration of the factors driving host-
88 symbiont associations in marine invertebrates.

89

90 2. RESULTS

91

92 2. 1 Two taxa dominate the *S. officinalis* microbiome.

93

94 We sampled 27 healthy adult cuttlefish (*Sepia officinalis*) from the mariculture laboratory
95 at Marine Biological Laboratory (Woods Hole, MA). The study comprised two time periods. The
96 first (20-21 June 2017) was a pilot survey in which three individuals were sampled. The second
97 (25 September -10 October 2017) was an experiment involving 24 individuals, of which 16 were
98 exposed to repeated doses of the antibiotic enrofloxacin and 8 individuals served as untreated
99 controls. 16S rRNA amplicon sequencing of the GI tract, gills, and skin of all 27 animals
100 revealed a highly simplified microbiota dominated by bacterial amplicon sequence variants
101 (ASVs) in the Vibrionaceae and Piscirickettsiaceae families, regardless of treatment with
102 enrofloxacin.

103 In particular, results showed a consistent and highly simplified microbiota in the
104 esophagus (Figure 1; Table 1). A single ASV in the genus *Vibrio* (referred to as ASV1 in
105 subsequent figures and tables) made up the majority of the 16S rRNA sequence data from the
106 esophagus of the three pilot investigation individuals (mean $92\% \pm 10\%$) and of 24 individuals
107 sampled four months later (control group mean $100\% \pm 1\%$; treatment group mean $94\% \pm 10\%$).
108 Thus, this ASV represents a dominant constituent of the esophagus microbiota stably over two
109 time periods in the study and after exposure to antibiotic treatment with enrofloxacin. Another
110 ASV of the related genus *Photobacterium* (Vibrionaceae) (referred to as ASV2 in Table 1) was
111 present in the esophagus community in the pilot investigation animals (mean $7\% \pm 10\%$).
112 Combined, the two Vibrionaceae ASVs (ASV1 and ASV2) in the three pilot animals constituted
113 $>99\%$ of the esophagus community.

114 The major *Vibrio* ASV1 was also a major constituent of downstream sites in the GI tract,
115 although present at lower abundance measured both as relative abundance in 16S sequencing

116 data and by quantitative PCR (qPCR) (Figure 1; Table 1). qPCR revealed a high abundance of
117 *Vibrio* cell copies in the esophagus (average 520.4 ± 410 copies/ng of total DNA including host
118 DNA) relative to more distal portions of the GI tract that included stomach, cecum, and intestine
119 (combined average 25.6 ± 77.8 copies/ng) ($p < 0.005$, $\chi^2 = 16.5$, df = 3 Kruskal-Wallis) (Fig. 1B).
120 Comparison of qPCR measures of ASVs in the genus *Vibrio* between the esophagus of treatment
121 and control animals revealed a striking and significant decrease of nearly 80% in the quantity (p
122 < 0.02 , df = 10.8, Welch two sample t-test). We did not observe a significant difference in *Vibrio*
123 ASV1 quantity between other organs of the digestive tract with antibiotic treatment (Fig. 1B).
124 Relative abundance of *Vibrio* ASV1 in the esophagus and stomach also did not differ
125 significantly between antibiotic and control groups (Welch two sample t-test, $p > 0.10$), but did
126 differ significantly among the cecum (Welch two sample t-test, $p = 0.00235$) and intestine
127 (Welch two sample t-test, $p = 1.99e-05$) of treatment versus control groups. Analysis of GI tracts
128 (esophagus, stomach, cecum, and intestine samples combined) between treated versus control
129 animals from the second period of study revealed significant differences in weighted UniFrac β -
130 diversity between the two groups (PERMANOVA $Pr(>F) = 0.006$, $F = 5.63$, df = 1), despite the
131 *Vibrio* ASV1 remaining dominant in most organs. These differences in measured relative
132 abundance and β -diversity may result from stochastic variation in low-abundance sequences, as
133 the non-*Vibrio* portion of the 16S rRNA sequence data from the GI tract consisted of an
134 assortment of taxa that varied between individuals or between the two time points of the study
135 and thus suggested transient organisms rather than stable microbial colonization.

136 Samples from gills were dominated by a single highly abundant ASV in the family
137 Piscirickettsiaceae (referred to as ASV3 in subsequent figures and tables), which made up an
138 average relative abundance of $96.9\% \pm 2.5\%$ in the gills. In samples from other body sites this

139 ASV3 was detected only sporadically and at low relative abundance (mean 0.2%, range 0 to
140 5.8%) (Fig. 1A). An additional Vibrio ASV, ASV4, was a major constituent of the microbiota of
141 the shrimp used as food for the cuttlefish and was also detectable in some samples from stomach,
142 cecum, and intestine (Figure 1A). Skin samples did not exhibit much similarity to GI tract or
143 gills with respect to microbiome composition, with most common ASVs found in other
144 anatomical sites comprising < 20% (mean $17.2\% \pm 2.9\%$) relative abundance of the
145 microbiome (Table S1).

146 In addition to surveying internal organs, we collected fecal samples from the 24 animals
147 from the second time period of our study. These samples were collected daily for each
148 individual throughout the course of the antibiotic treatment experiment (see methods).
149 Comparison of weighted UniFrac dissimilarity of fecal samples from experimental animals
150 revealed significant differences in beta-diversity between cuttlefish fecal samples, seawater, and
151 shrimp (PERMANOVA $\text{Pr}(>F) = 0.001$, $F = 5.26$, $\text{df} = 2$) upon which the animals were fed.
152 These results, paired with the differences we observed in compositional relative abundance
153 between organs, seawater, and shrimp provide additional support for our finding that bacterial
154 communities associated with cuttlefish differ from those found in their seawater environment and
155 food source (Fig. 2).

156

157

158 2.2 Imaging shows spatial structure of the microbiota in cuttlefish esophagus and scattered
159 distribution elsewhere in the gastrointestinal tract.

160

161 Fluorescence *in situ* hybridization (FISH) revealed a striking organization of bacteria
162 distributed in a layer lining the interior of the convoluted esophagus of cuttlefish (Fig. 3A-C).
163 Hybridization with the near-universal Eub338 probe showed bacteria in high density in a layer
164 ~20-40 μ m thick at the border between host tissue and lumen. Staining with fluorophore-
165 conjugated wheat germ agglutinin revealed a mucus layer that covered the epithelium and
166 generally enclosed the bacteria (Fig. 3). To verify the identity of these bacteria we employed a
167 nested probe set including Eub338 as well as probes for Alphaproteobacteria,
168 Gammaproteobacteria, and probes we designed specifically for Vibrionaceae (Vib1749 and
169 Vib2300, Table 2). Bacterial cells imaged in the esophagus showed signal from all probes
170 expected to hybridize with Vibrionaceae, suggesting that the bacteria observed in this organ are a
171 near-monoculture of this taxon (Fig. 4B-E). A probe targeted to Alphaproteobacteria was
172 included in the FISH as a negative control and, as expected, did not hybridize with the cells (Fig.
173 4F). As an additional control to detect non-specific binding of probes, we performed an
174 independent FISH with a set of probes labeled with the same fluorophores as the experimental
175 probe set but conjugated to oligonucleotides not expected to hybridize with the cuttlefish
176 microbiota (Table 2). No signal from this non-target probe set was detected (Fig. 4G-H)
177 supporting the interpretation that the signal observed in the esophagus results from a specific
178 interaction of the Vibrionaceae-targeted oligonucleotides with the visualized bacteria.
179 In other parts of the digestive tract we observed a sparser distribution of bacteria without
180 obvious spatial organization. Bacteria in the intestine were present not in a layer but scattered
181 throughout the lumen and mixed with the luminal contents (Fig. 5). Similarly, in the cecum, we
182 observed bacteria in low abundance in the lumen (Fig. 6). FISH was also applied to the stomach,

183 posterior salivary gland (poison gland) and duct of the salivary gland, but no bacteria were
184 detected (not shown).

185 Fluorescence *in situ* hybridization to cross-sections of the gills revealed clusters of
186 bacteria at or near the surface of the tissue (Fig. 7). These bacteria hybridized with the Eub338
187 near-universal probe and a probe for Gammaproteobacteria (Fig. 7B, C, Table 2) but not
188 Alphaproteobacteria (not shown), consistent with the identification of the clusters of gill bacteria
189 as members of the gammaproteobacterial family Piscirickettsiaceae.

190

191 3. DISCUSSION

192

193 We sampled the cuttlefish microbiome of the digestive tract, gills, and skin and found
194 dense colonization of an unexpected site, the esophagus, by a bacterium of the genus *Vibrio*.
195 Both imaging and 16S rRNA gene sequencing showed a near-monoculture of *Vibrionaceae* in
196 the esophagus, with imaging showing dense colonization of the interior lining of the esophagus
197 with a single morphotype that hybridized to probes targeting *Vibrionaceae*. In the remainder of
198 the GI tract, both imaging and 16S rRNA sequencing indicated a less consistent microbiota.
199 Sequencing also showed lower relative abundance of the dominant *Vibrio* ASV, and qPCR
200 confirmed a significantly lower total abundance of *Vibrio* cell copies in the distal GI tract.
201 Imaging revealed sparse and sporadic colonization in the intestine and cecum, with scattered
202 cells in the lumen and no clear colonization of the epithelium. In light of these results, we
203 conclude that the GI tract of laboratory cultured *Sepia officinalis* has a highly simplified
204 microbiome dominated by the genus *Vibrio*.

205 Diverse associations with *Vibrio* and the Vibrionaceae are known from cephalopods.
206 Among the most extensively investigated is the mutualistic association of the bioluminescent
207 *Vibrio (Aliivibrio) fischeri* with the light organ of the bobtail squid *Euprymna scolopes* (1, 13).
208 Other well-known symbioses include the colonization of the cephalopod accessory nidamental
209 gland with Alpha- and Gammaproteobacteria, which enables the host to secrete a layer of
210 bacteria into the protective coating of the egg capsule (3, 14-18). Thus, colonization by
211 Gammaproteobacteria and specifically by Vibrionaceae is common in cephalopods, yet
212 colonization of the GI tract, and particularly the esophagus, was unexpected.

213 Bacteria from genus *Vibrio* and the related Vibrionaceae genus *Photobacterium* are
214 frequent colonizers of the GI tracts of marine fishes (19, 20) and are prominent in the
215 gastrointestinal microbiota of *Octopus vulgaris* paralarvae (21). Vibrionaceae have been reported
216 to produce chitinases, proteases, amylase, and lipase (20), suggesting the possibility that
217 colonization of the digestive tract by the Vibrionaceae serves to aid in host digestion (20). If the
218 *Vibrio* and *Photobacterium* ASVs serve this function, their localization in high density in the
219 esophagus, near the beginning of the digestive tract, may serve to seed the distal gut;
220 colonization of the lining of the esophagus may provide a reservoir that permits the microbes to
221 avoid washout from the gut by continually re-populating the lumen of downstream gut chambers.

222 An alternative explanation is that the colonization of the esophagus, and the rest of the
223 gut, is pathogenic or opportunistic. Various *Vibrio* species are known pathogens of cephalopods,
224 causing skin lesions and sometimes mortality in squids and octopuses (22-24). The genus *Vibrio*
225 includes representative species that are pathogenic to corals (*V. corallilyticus*), fish (*V.*
226 *salmonicida*), diverse marine organisms (*V. harveyi*) and humans (*V. alginolyticus*, *V. cholerae*,
227 *V. parahaemolyticus*, and *V. vulnificus*) (25, 26). Likewise, the genus *Photobacterium* contains

228 pathogenic as well as commensal representatives (27). A previous study of the microbiota of
229 *Octopus vulgaris* paralarvae found that recently hatched paralarvae had a high-diversity
230 microbiome that changed, in captivity, to a lower-diversity microbiome with abundant
231 Vibrionaceae (21). Whether the Vibrionaceae are an integral part of cuttlefish physiology in
232 nature or whether they represent opportunistic colonists of these laboratory-reared organisms is a
233 question for future research.

234 Our sequence data from gills were dominated by a single ASV classified as
235 Piscirickettsiaceae that was in low abundance at other body sites. The Piscirickettsiaceae are a
236 family within the Gammaproteobacteria (28) that includes the salmon pathogen *P. salmonis*.
237 Rickettsia-like organisms have been described from the gills of clams and oysters (29, 30) as
238 well as associated with the copepod *Calanus finmarchicus* (31). In recent years
239 Piscirickettsiaceae have been identified in high-throughput sequencing datasets from seawater
240 and sediment as a taxon that may be involved in biodegradation of oil and other compounds (32-
241 38). Whether taxa in this family colonize the gills of cuttlefish and other organisms as symbionts
242 or as opportunistic pathogens is a subject for future investigation.

243 Studies of wild *S. officinalis* microbiota will be informative for understanding natural
244 host-symbiont associations under natural conditions, as compared to the mariculture-reared
245 animals in the present study. *S. officinalis* in the eastern Atlantic and Mediterranean are known to
246 prey on small mysids (crustaceans) in their first few weeks post-hatching; then as juveniles and
247 adults they prey mainly on marine fishes and crabs. The sparseness and simplicity of the gut
248 microbiota observed in our study may have been in part a result of the monodiet of grass shrimp
249 (*Palaemonetes*) we employed. It remains to be seen whether differences in diet and natural

250 variation in environmental conditions influence the association of microbial symbionts with *S.*
251 *officinalis* in the wild.

252 Because cuttlefish behavior is well-studied and there exist standardized methods for
253 documenting multiple behaviors (8), we hypothesized that these animals may provide a unique
254 opportunity to study microbes and the gut-brain axis – the effect of gut microbiota on behavior
255 (39) – in an invertebrate system. Therefore, in parallel with our study of the microbiome of
256 various organ systems, we conducted extensive preliminary experiments to study the effect of
257 antibiotic treatment on the behavior of *S. officinalis*. These results were largely negative, perhaps
258 due to the highly simplified microbiota we observed and its resilience to the antibiotic employed.
259 These results may prove helpful to the cephalopod husbandry community, as they suggest that
260 application of the commonly used antibiotic enrofloxacin is compatible with maintenance of
261 normal behavioral and microbiome characteristics of this species

262

263

264 **4. MATERIALS AND METHODS**

265

266 **4. 1 Sampling and antibiotic treatment**

267

268 Our study included 27 cuttlefish that were bred in the wild and moved to captivity prior
269 to hatching. Animals were held in water tables connected to a single open-filtration system fed
270 by filtered seawater. Animals were euthanized via immersion into a 10% dilution of ethanol in
271 seawater and were then dissected under sterile conditions within a biosafety cabinet using
272 autoclaved tools to obtain samples for microbial analyses. The gastrointestinal tract was

273 dissected into four components: esophagus, stomach, cecum, and intestine. Gill tissue and skin
274 from the mantle was sampled as well (~ 0.5g per sample). All tissues were stored in separate
275 sterile cryogenic tubes and flash-frozen in liquid nitrogen.

276 Following a pilot study of three individual cuttlefish, we included 24 cuttlefish (16 test, 8
277 control) in an experiment designed to test the effect of the antibiotic treatment on the
278 composition of the cuttlefish microbiome. The experimental design consisted of administering
279 antibiotic to animals in the treatment group (n = 16) via injection into the food source (grass
280 shrimp, *Palaemonetes* sp.), which was then fed to the animals. Prior to feeding, shrimp were
281 injected with enrofloxacin (Baytril®; 22.7 mg/mL, Bayer HealthCare LLC, Shawnee Mission,
282 KS, USA) using a 0.5 cc, U-100 insulin syringe with an attached 28 g x 1/2" needle (Covidien
283 LLC, Mansfield, MA, USA). The antibiotic dosage was 10 mg/kg rounded up to the nearest
284 hundredth mL. The antibiotic was injected into the coelomic cavity of the shrimp which were
285 then immediately fed to the cuttlefish once daily for 14 days. We maintained 8 animals as
286 controls, none of which received antibiotic treatment. Experimental animals were held in two
287 separate water tables and control animals a third, all of which were connected to the same open-
288 filtration system fed by filtered seawater. Within each water table, animals were isolated into
289 individual holding pens via plastic panels. The experimental period lasted for 14 days (1 – 15
290 Oct 2017), during which fecal samples were collected from each individual daily; fecal samples
291 were collected via pipetting free-floating material from the tank of each individual animal into a
292 sterile pipette.

293 To assess the extent to which cuttlefish microbial symbionts were shared with their
294 environment and food sources, 1L water samples were taken from each of three water tables in
295 which animals were held on the day of euthanasia and filtered using a 0.22 micron Sterivex filter

296 for DNA extraction; grass shrimp used as the food source throughout the duration of the
297 experiment were collected in 1.8ml sterile cryotubes on the same day that water was sampled,
298 and were frozen at -20°C until prepared for DNA extraction.

299

300

301 4.2 DNA extraction, sequencing, qPCR, and 16S rRNA gene statistical analyses

302

303 DNA extractions were performed on cuttlefish tissue biopsies, water, and whole shrimp
304 using the MoBio PowerSoil 96 Well Soil DNA Isolation Kit (Catalog No. 12955-4, MoBio,
305 Carlsbad, CA, USA). We used the standard 515f and 806r primers (49-51) to amplify the V4
306 region of the 16S rRNA gene, using mitochondrial blockers to reduce amplification of host
307 mitochondrial DNA. Sequencing was performed using paired-end 150 base reads on an
308 Illumina HiSeq sequencing platform. Following standard demultiplexing and quality filtering
309 using the Quantitative Insights Into Microbial Ecology pipeline (QIIME2) (52) and vsearch8.1
310 (53), ASVs were identified using the Deblur method (19) and taxonomy was assigned using the
311 Greengenes Database (May 2013 release; <http://greengenes.lbl.gov>). Libraries containing fewer
312 than 1000 reads were removed from further analyses. All 16S rRNA sequence data and metadata
313 will be made available via the QIITA platform prior to publication. Statistical analyses and
314 figure production were produced with the aid of several R packages including vegan (40), dplyr
315 (41), ggplot2 (42) and Adobe Illustrator® CC 2019. Code for analyses and figures is available at
316 www.github.com/hollylutz/CuttlefishMP. We performed qPCR analyses targeting the genus
317 *Vibrio* to quantify the abundance of bacterial cells throughout the GI tract. Conditions for qPCR
318 were borrowed from Thompson et al. (43), using the primers 567F and 680R and performing two

319 replicates of qPCR analysis that were combined to produce the final results reported in this
320 study.

321

322 4.3 Sample collection, fixation and sectioning for imaging

323

324 Samples from esophagus, stomach, intestine and cecum of 9 cuttlefish (1 from the pilot
325 and 8 from the second period experiment) were dissected and divided in order to include the
326 same individuals in both microscopy and sequencing analyses. Immediately after dividing,
327 samples for imaging were fixed with 2% paraformaldehyde in 10 mM Tris pH 7.5 for 12 h at 4
328 °C, washed in PBS, dehydrated through an ethanol series from 30, 50, 70, 80 and 100%, and
329 stored at -20 °C. Samples were dehydrated with acetone for 1 h, infiltrated with Technovit 8100
330 glycol methacrylate (EMSdiasum.com) infiltration solution 3 times 1 hour each followed by a
331 final infiltration overnight under vacuum, transferred to Technovit 8100 embedding solution and
332 solidified for 12 h at 4 °C. Blocks were sectioned to 5 um thickness and applied to Ultrastick
333 slides (Thermo Scientific). Sections were stored at room temperature until FISH was performed.

334

335 4.4 Fluorescence *in situ* hybridization (FISH)

336

337 Hybridization solution [900 mM NaCl, 20 mM Tris, pH 7.5, 0.01% SDS, 20% (vol/vol)
338 formamide, each probe at a final concentration of 2 µM] was applied to sections and incubated at
339 46 °C for 2 h in a chamber humidified with 20% (vol/vol) formamide. Slides were washed in
340 wash buffer (215 mM NaCl, 20 mM Tris, pH 7.5, 5mM EDTA) at 48 °C for 15 min. Samples
341 were incubated with wheat germ agglutinin (20 ug ml⁻¹) conjugated with Alexa Fluor 488 and

342 DAPI (1 ug ml⁻¹) at room temperature for 30 minutes after FISH hybridization to label mucus
343 and host nuclei, respectively. Slides were dipped in ice-cold deionized water, air dried, mounted
344 in ProLong Gold antifade reagent (Invitrogen) with a #1.5 coverslip, and cured overnight in the
345 dark at room temperature before imaging. Probes used in this study are listed in Table 2.

346

347 4.5 Image acquisition and linear unmixing

348

349 Spectral images were acquired using a Carl Zeiss LSM 780 confocal microscope with a
350 Plan-Apochromat 40X, 1.4 N.A. objective. Images were captured using simultaneous excitation
351 with 405, 488, 561, and 633 nm laser lines. Linear unmixing was performed using the Zeiss ZEN
352 Black software (Carl Zeiss) using reference spectra acquired from cultured cells hybridized with
353 Eub338 probe labeled with the appropriate fluorophore and imaged as above. Unmixed images
354 were assembled and false-colored using FIJI software (Schindelin *et al.*, 2012).

355

356 4.6 Data availability

357 All 16S rRNA sequences and sample metadata will be made available via the QIITA platform
358 prior to publication.

359

360 FIGURE LEGENDS

361

362 **Figure 1. A single *Vibrio* taxon dominates the esophagus, and a single *Piscirickettsiaceae***
363 **taxon dominates the gills of the European common cuttlefish in captivity. (A)** Relative
364 abundance of top bacterial taxa found among cuttlefish organs. Shrimp for feeding and seawater

365 from holding tanks are also shown. ASVs are labeled according to the finest level of taxonomic
366 resolution provided by the Greengenes database; bacteria not included in the top 8 taxa are
367 pooled as “other”. Bars correspond to individual 16S rRNA sequence libraries from the pilot
368 investigation animals (labeled “A”), experimental animals in the control category (labeled “B”),
369 and experimental animals in the antibiotic treatment category (labeled “C”); only libraries with
370 >1000 read depth are shown. (B) Quantity of *Vibrio* cells per nanogram of DNA measured using
371 *Vibrio*-specific primers (567F and 680R (43)). Asterisk indicates significant difference between
372 organs ($p < 0.05$, Welch two sample t-test). (C) Anatomical depiction of the gastrointestinal tract
373 of *S. officinalis*, illustration modified from Plate XI of Tompsett (44).

374

375 **Figure 2. Principal Coordinates Analysis (PCoA) of weighted UniFrac β -diversity**
376 comparing shrimp, tank water, and (A) fecal samples of treatment cuttlefish and (B) fecal
377 samples of control cuttlefish. Fecal samples from control animals (B) show a more tightly
378 clustered pattern than do fecal samples from animals treated with enrofloxacin (A).

379

380 **Figure 3. Spatial organization of bacteria in the esophagus of the European common**
381 **cuttlefish, *S. officinalis*.** The image shown is a cross-section of esophagus that was embedded in
382 methacrylate, sectioned, and subjected to fluorescence *in situ* hybridization (FISH). (A) Bacteria
383 (magenta) lining the interior of the esophagus in association with the mucus layer (wheat germ
384 agglutinin staining, green). (B) and (C) are enlarged images of the regions marked with
385 arrowheads in (A) where bacteria extend past the edge of the mucus layer. Blue: Host nuclei.
386 Scale bar =100 μm (A); 20 μm (B) and (C).

387

388 **Figure 4. Fluorescence *in situ* hybridization identifies bacteria in the esophagus of *S.***
389 ***officinalis* as Vibrionaceae.** A methacrylate-embedded section was hybridized with a nested
390 probe set containing probes for most bacteria, Gammaproteobacteria, Alphaproteobacteria, and
391 Vibrionaceae. (A) near-universal probe showing a similar bacterial distribution as in Figure 3.
392 (B, C, D) Enlarged images of the region marked by the dashed square in (A) showing
393 hybridization with near-universal, Vibrionaceae, and Gammaproteobacteria probes, respectively.
394 (E) Merged image of B, C, and D showing an exact match of the signal from those three probes.
395 (F) Alphaproteobacteria probe showing no hybridization. (G) An independent hybridization with
396 the non-target probe set as a control; no signal is observed. (H) enlarged image of the dashed
397 square in (G). Scale bar=20 μ m (A, G); 5 μ m (B-F, H).

398
399 **Figure 5. Fluorescence *in situ* hybridization in intestine of *S. officinalis*.** A methacrylate-
400 embedded section was hybridized with the near-universal probe and stained with fluorophore-
401 labeled wheat germ agglutinin to visualize mucus. (A) Bacteria (magenta) are sparsely
402 distributed through the lumen. (B) Enlarged image of the dashed square in (A). (C) An
403 independent FISH control with a non-target probe (Hhaem1007); no signal was detected. Scale
404 bar= 20 μ m (A, C); 5 μ m (B).

405
406 **Figure 6. Fluorescence *in situ* hybridization in cecum of *S. officinalis*.** (A) Bacteria are
407 observed in low abundance in the lumen of cecum. (B) Enlarged image of dashed square in (A).
408 Scale bar=20 μ m (A); 5 μ m (B).

409

410 **Figure 7. Fluorescence *in situ* hybridization in gills of *S. officinalis*.** Bacteria are observed in
411 small clusters at or near the surface of the gill. (A) Overview image. (B, C): enlarged images of
412 the dashed square in (A) showing hybridization with near-universal and Gammaproteobacteria
413 probes, respectively. (D) Merged image of (B) and (C) showing colocalization of the signal from
414 those two probes. Scale bar=20 μ m (A); 5 μ m (B-D).

415

416

417 **ACKNOWLEDGEMENTS**

418 We thank Alan Kuzirian, Louie Kerr, Wyatt Arnold, Madeline Kim, Elle Hill, Tyler He, Tifani
419 Anton, and Eric Edsinger. HLL was supported by NSF 1611948. TR and JMW were supported
420 by NSF 1650141. RTH thanks the Sholley Foundation for partial support. Amber Durand was
421 supported by the Woods Hole Partnership Education Program. The funders had no role in study
422 design, data collection and interpretation, or the decision to submit the work for publication.

423

424

425

426

427

428 **REFERENCES**

429

430 1. **McFall-Ngai M.** 2014. Divining the essence of symbiosis: insights from the squid-vibrio
431 model. PLoS Biol **12**:e1001783.

432 2. **Kerwin AH, Nyholm SV.** 2017. Symbiotic bacteria associated with a bobtail squid
433 reproductive system are detectable in the environment, and stable in the host and
434 developing eggs. Environ Microbiol **19**:1463-1475.

435 3. **Barbieri E, Bruce J. Paster, Deborah Hughes, Ludek Zurek, Duane P. Moser, Andreas**
436 **Teske, and Mitchell L. Sogin** 2001. Phylogenetic characterization of epibiotic bacteria in
437 the accessory nidamental gland and egg capsules of the squid *Loligo pealei*
438 (Cephalopoda: Loliginidae). *Environmental Microbiology* **3**:151-167.

439 4. **Iehata S, Valenzuela F, Riquelme C.** 2016. Evaluation of relationship between Chilean
440 octopus (*Octopus mimus*Gould, 1852) egg health condition and the egg bacterial
441 community. *Aquaculture Research* **47**:649-659.

442 5. **Panetta D, Solomon M, Buresch K, Hanlon RT.** Small-scale rearing of cuttlefish (*Sepia*
443 *officinalis*) for research purposes. *Marine and Freshwater Behaviour and Physiology*
444 **50**:115-124.

445 6. **Messenger JB.** 2001. Cephalopod chromatophores: neurobiology and natural history.
446 *Biological Review* **76**:473-528.

447 7. **Darmaillacq AS, Dickel L, Mather J.** 2014. Cephalopod cognition. Cambridge University
448 Press, Cambridge, UK.

449 8. **Hanlon RT, Messenger JB.** 1988. Adaptive coloration in young cuttlefish (*Sepia officinalis*
450 *L*): the morphology and development of body patterns and their relation to behaviour.
451 *Phil Trans R Soc B* **320**:437-487.

452 9. **Buresch KC, Ulmer KM, Akkaynak D, Allen JJ, Mäthger LM, Nakamura M, Hanlon RT.**
453 2015. Cuttlefish adjust body pattern intensity with respect to substrate intensity to aid
454 camouflage, but do not camouflage in extremely low light. *Journal of Experimental*
455 *Marine Biology and Ecology* **462**:121-126.

456 10. **Yu C, Li Y, Zhang X, Huang X, Malyarchuk V, Wang S, Shi Y, Gao L, Su Y, Zhang Y, Xu H,**
457 **Hanlon RT, Huang Y, Rogers JA.** 2014. Adaptive optoelectronic camouflage systems with
458 designs inspired by cephalopod skins. *Proc Natl Acad Sci U S A* **111**:12998-13003.

459 11. **Chiao CC, Chubb C, Hanlon RT.** 2015. A review of visual perception mechanisms that
460 regulate rapid adaptive camouflage in cuttlefish. *Journal of Comparative Physiology A: Neuroethology, Sensory, Neural, and Behavioral Physiology* **201**:933-945.

462 12. **Tonkins BM, Tyers AM, Cooke GM.** 2015. Cuttlefish in captivity: An investigation into
463 housing and husbandry for improving welfare. *Applied Animal Behaviour Science*
464 **168**:77-83.

465 13. **Koch EJ, Miyashiro T, McFall-Ngai MJ, Ruby EG.** 2014. Features governing symbiont
466 persistence in the squid-vibrio association. *Molecular Ecology* **23**:1624-1634.

467 14. **Bloodgood RA.** 1977. The squid accessory nidamental gland: ultrastructure and
468 association with bacteria. . *Tissue & Cell* **9**:197-208.

469 15. **Pichon D, Isabelle Domart-Coulon, and Renata Boucher-Rodoni** 2017. Cephalopod
470 bacterial associations: characterization and isolation of the symbiotic complex in the
471 Accessory Nidamental Glands. . *Boll Malacol* **43**:96-102.

472 16. **Collins AJ, LaBarre BA, Won BS, Shah MV, Heng S, Choudhury MH, Haydar SA, Santiago**
473 **J, Nyholm SV.** 2012. Diversity and partitioning of bacterial populations within the
474 accessory nidamental gland of the squid *Euprymna scolopes*. *Appl Environ Microbiol*
475 **78**:4200-4208.

476 17. **Gromek SM, Andrea M. Suria, Matthew S. Fullmer, Jillian L. Garcia, Johann Peter**
477 **Gogarten, Spencer V. Nyholm, and Marcy J. Balunas.** 2016. *Leisingera* sp. JC12, a

478 Bacterial Isolate from Hawaiian Bobtail Squid Eggs, Produces Indigoidine and
479 Differentially Inhibits Vibrios. *Frontiers in Microbiology* **7**:1342.

480 18. **Lum-Kong A, Hastings TS.** 1992. The accessory nidamental glands of *Loligo forbesi*
481 (Cephalopoda: Loliginidae): characterization of symbiotic bacteria and preliminary
482 experiments to investigate factors controlling sexual maturation. *J Zool, Lond* **228**:395-
483 403.

484 19. **Tarnecki AM, Burgos FA, Ray CL, Arias CR.** 2017. Fish intestinal microbiome: diversity
485 and symbiosis unravelled by metagenomics. *J Appl Microbiol* doi:10.1111/jam.13415.

486 20. **Egerton S, Sarah Culloty, Jason Whooley, Catherine Stanton, and R. Paul Ross** 2018.
487 The Gut Microbiota of marine fish. *Microbiology* **9**:837.

488 21. **Roura A, Doyle SR, Nande M, Strugnell JM.** 2017. You Are What You Eat: A Genomic
489 Analysis of the Gut Microbiome of Captive and Wild *Octopus vulgaris* Paralarvae and
490 Their Zooplankton Prey. *Front Physiol* **8**:362.

491 22. **Hanlon RT, Forsythe JW.** 1990. 1. Diseases of Mollusca: Cephalopoda. 1.1. Diseases
492 caused by microorganisms and 1.3 Structural abnormalities and neoplasia., p 23-46 and
493 203-204. *In Kinne O (ed), Diseases of Marine Animals, vol III. Biologische Anstalt
494 Helgoland, Hamburg.*

495 23. **Forsythe JW, Hanlon RT, Lee PG.** 1990. A formulary for treating cephalopod mollusc
496 diseases. San Diego: Academic Press.

497 24. **Ford LA, Alexander SK, Cooper KM, Hanlon RT.** 1986. Bacterial populations of normal
498 and ulcerated mantle tissue of the squid, *Loliguncula brevis*. *Journal of Invertebrate
499 Pathology* **48**:13-26.

500 25. **Takemura AF, Chien DM, Polz MF.** 2014. Associations and dynamics of Vibrionaceae in
501 the environment, from the genus to the population level. *Front Microbiol* **5**:38.

502 26. **Pruzzo C, Huq A, Colwell RR, Donelli G.** 2005. Pathogenic Vibrio Species in the Marine
503 and Estuarine Environment, p 217-252. *In Belkin S, Colwell RR (ed), Oceans and Health:
504 Pathogens in the Marine Environment* doi:10.1007/0-387-23709-7_9. Springer US,
505 Boston, MA.

506 27. **Labela AM, Arahal DR, Castro D, Lemos ML, Borrego JJ.** 2017. Revisiting the genus
507 *Photobacterium*: taxonomy, ecology and pathogenesis. *Int Microbiol* **20**:1-10.

508 28. **Mauel MJ, S.J. Giovannoni, and J.L. Fryer** 1999. Phylogenetic analysis of *Piscirickettsia*
509 *salmonis* by 16S, internal transcribed spacer (ITS) and 23S ribosomal DNA sequencing. *Diseases of
510 Aquatic Organisms* **35**:115-123.

511 29. **Azevedo C, Villalba A.** Extracellular Giant Rickettsiae Associated with Bacteria in the Gill
512 of *Crassostrea gigas* (Mollusca, Bivalvia). *Journal of Invertebrate Pathology* **58**:75-81.

513 30. **Wen C-M, Guang-Hsiung Kou, and Shiu-Nan Chen** 1994. Rickettsiaceae-like
514 Microorganisms in the Gill and Digestive Gland of the Hard Clam, *Meretrix lusoria*
515 Röding. *Journal of Invertebrate Pathology* **64**:138-142.

516 31. **Moisander P, Andrew D. Sexton, and Meaghan C. Daley.** 2014. Stable Associations
517 Masked by Temporal Variability in the Marine Copepod Microbiome. *PLoS ONE*
518 **10**:e0138967.

519 32. **Lu X, Sun S, Hollibaugh JT, Mou X.** 2015. Identification of polyamine-responsive
520 bacterioplankton taxa in South Atlantic Bight. *Environ Microbiol Rep* **7**:831-838.

521 33. **Wang K, Zhang D, Xiong J, Chen X, Zheng J, Hu C, Yang Y, Zhu J.** 2015. Response of
522 bacterioplankton communities to cadmium exposure in coastal water microcosms with
523 high temporal variability. *Appl Environ Microbiol* **81**:231-240.

524 34. **Hamdan LJ, Salerno JL, Reed A, Joye SB, Damour M.** 2018. The impact of the Deepwater
525 Horizon blowout on historic shipwreck-associated sediment microbiomes in the
526 northern Gulf of Mexico. *Sci Rep* **8**:9057.

527 35. **Kamalanathan M, Xu C, Schwehr K, Bretherton L, Beaver M, Doyle SM, Genzer J,**
528 **Hillhouse J, Sylvan JB, Santschi P, Quigg A.** 2018. Extracellular Enzyme Activity Profile in
529 a Chemically Enhanced Water Accommodated Fraction of Surrogate Oil: Toward
530 Understanding Microbial Activities After the Deepwater Horizon Oil Spill. *Front
531 Microbiol* **9**:798.

532 36. **Lofthus S, Netzer R, Lewin AS, Heggeset TMB, Haugen T, Brakstad OG.** 2018.
533 Biodegradation of n-alkanes on oil-seawater interfaces at different temperatures and
534 microbial communities associated with the degradation. *Biodegradation* **29**:141-157.

535 37. **Ribicic D, McFarlin KM, Netzer R, Brakstad OG, Winkler A, Throne-Holst M, Storseth
536 TR.** 2018. Oil type and temperature dependent biodegradation dynamics - Combining
537 chemical and microbial community data through multivariate analysis. *BMC Microbiol*
538 **18**:83.

539 38. **Wang B, Liu H, Tang H, Hu X.** 2018. Microbial ecological associations in the surface
540 sediments of Bohai Strait. *Journal of Oceanology and Limnology* **36**:795-804.

541 39. **Carabotti M, Scirocco A, Maselli MA, Severi C.** 2015. The gut-brain axis: interactions
542 between enteric microbiota,
543 central and enteric nervous systems. *Annals of Gastroenterology* **28**:203-209.

544 40. **Oksanen J., Blanchet F. G., Friendly M., Kindt R., Legendre P., McGlinn D., Minchin P.
545 R., O'Hara R. B., Simpson G. L., Solymos P., Henry M., Stevens H., Szoecs E., H. W.
546 2018. vegan: Community Ecology Package, vR package version 2.5-2.** <https://CRAN.R-project.org/package=vegan>.

547 41. **Wickham H, François R, Henry L, Müller K.** 2018. dplyr: A Grammar of Data
549 Manipulation, vR package version 0.7.6. <https://CRAN.R-project.org/package=dplyr>.

550 42. **Wickham H.** 2016. *ggplot2: Elegant Graphics for Data Analysis*. Springer-Verlag, New
551 York, NY.

552 43. **Thompson J, Randa M, Marcelino L, Tomita-Mitchell A, Lim E, Polz M.** 2004. Diversity
553 and dynamics of a north Atlantic coastal *Vibrio* community. *Applied Environmental
554 Microbiology* **70**:4103-4110.

555 44. **Tompsett DH.** 1939. *L. M. B. C. Memoirs on Typical British Marine Plants & Animals*. The
556 University Press of Liverpool.

557

558 42. **Amann RI, Ludwig W., Schleifer, K.** 1995. Phylogenetic identification and in situ
559 detection of individual microbial cells without cultivation. *Microbiological Reviews* **59**:143-169.

560

561 43. **Neef A.** 1997. Anwendung der in situ-Einzelzell- Identifizierung von Bakterien zur
562 Populations analyse in komplexen mikrobiellen BiozönosenUniversity of Munich.

563

564 44. **Manz W, Amann R, Ludwig W, Wagner M, Schleifer KH.** 1992. Phylogenetic
565 oligodeoxynucleotide probes for the major subclasses of Proteobacteria: problems and
566 solutions. *Systematic and Applied Microbiology* **15**:593-600.

567

568 45. **Chalmers NI, Palmer RJ, Jr., Cisar JO, Kolenbrander PE.** 2008. Characterization of a
569 *Streptococcus* sp.-*Veillonella* sp. community micromanipulated from dental plaque. *J*
570 *Bacteriol* **190**:8145-8154.

571

572 46. **Valm A. M. MW, J. L., Rieken, C. W., Hasegawa, Y., Sogin, M. L., Oldenbourg, R.,**
573 **Dewhirst, F. E., Borisy, G. G. .** 2011. Systems-level analysis of microbial community
574 organization through combinatorial labeling and spectral imaging.

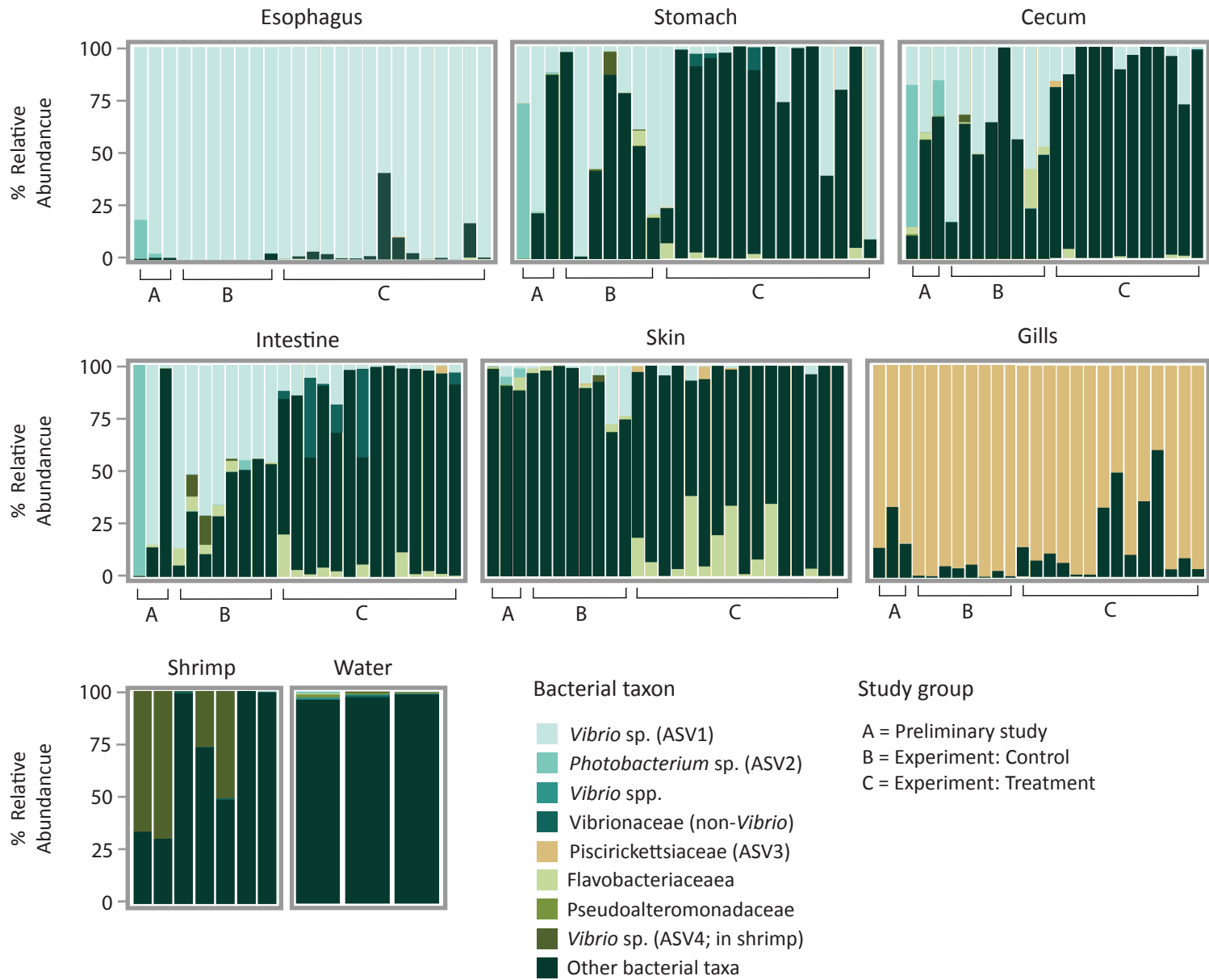
575

576

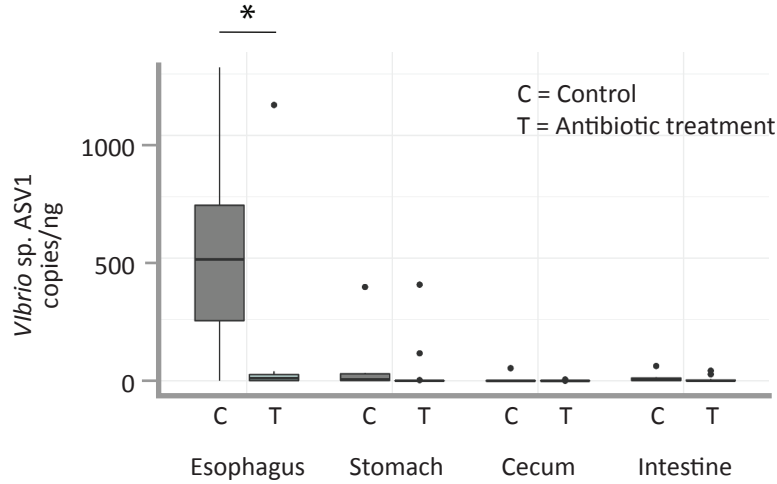
577

578

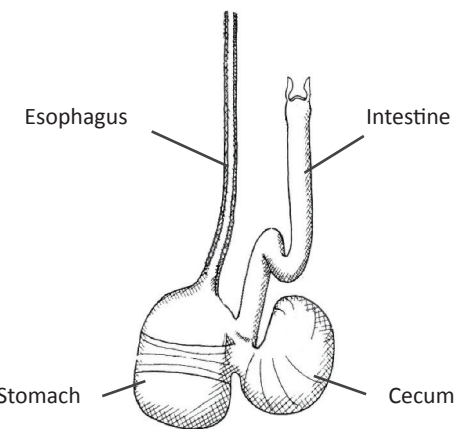
A



B

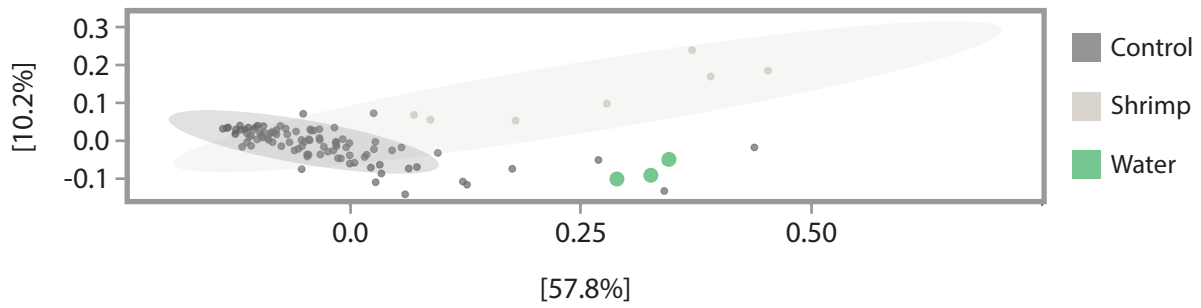


C



A

Control Group Fecal vs Shrimp, Water



B

Treatment Group Fecal vs Shrimp, Water

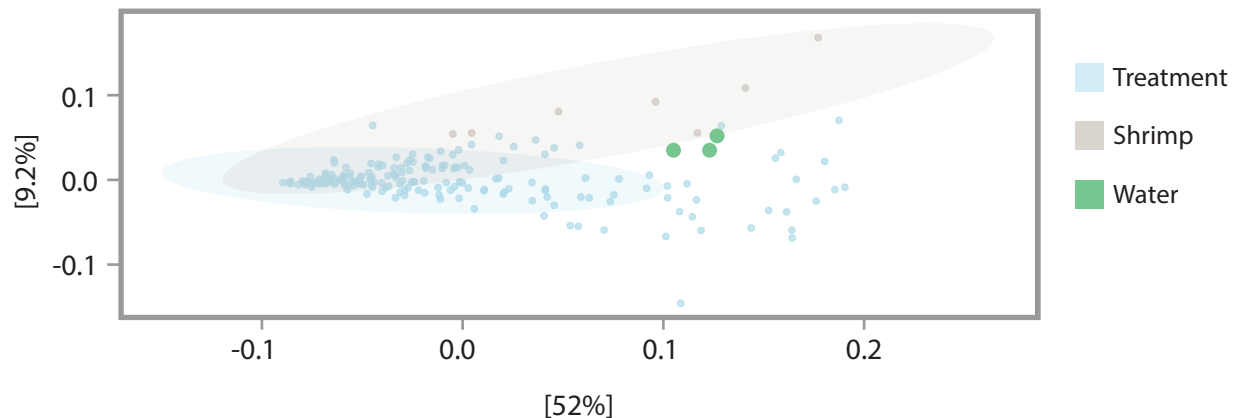


Figure 3. Spatial organization of bacteria in the esophagus of *S. officinalis*. The image shown is a cross-section of esophagus that was embedded in methacrylate, sectioned, and subjected to fluorescence *in situ* hybridization. (A) Bacteria (magenta) lining the interior of the esophagus in association with the mucus layer (wheat germ agglutinin staining, green). (B) and (C) are enlarged images of the regions marked with arrowheads in (A) where bacteria extend past the edge of the mucus layer. Blue: Host nuclei. Scale bar =100 μ m in (A) and 20 μ m in (B) and (C).

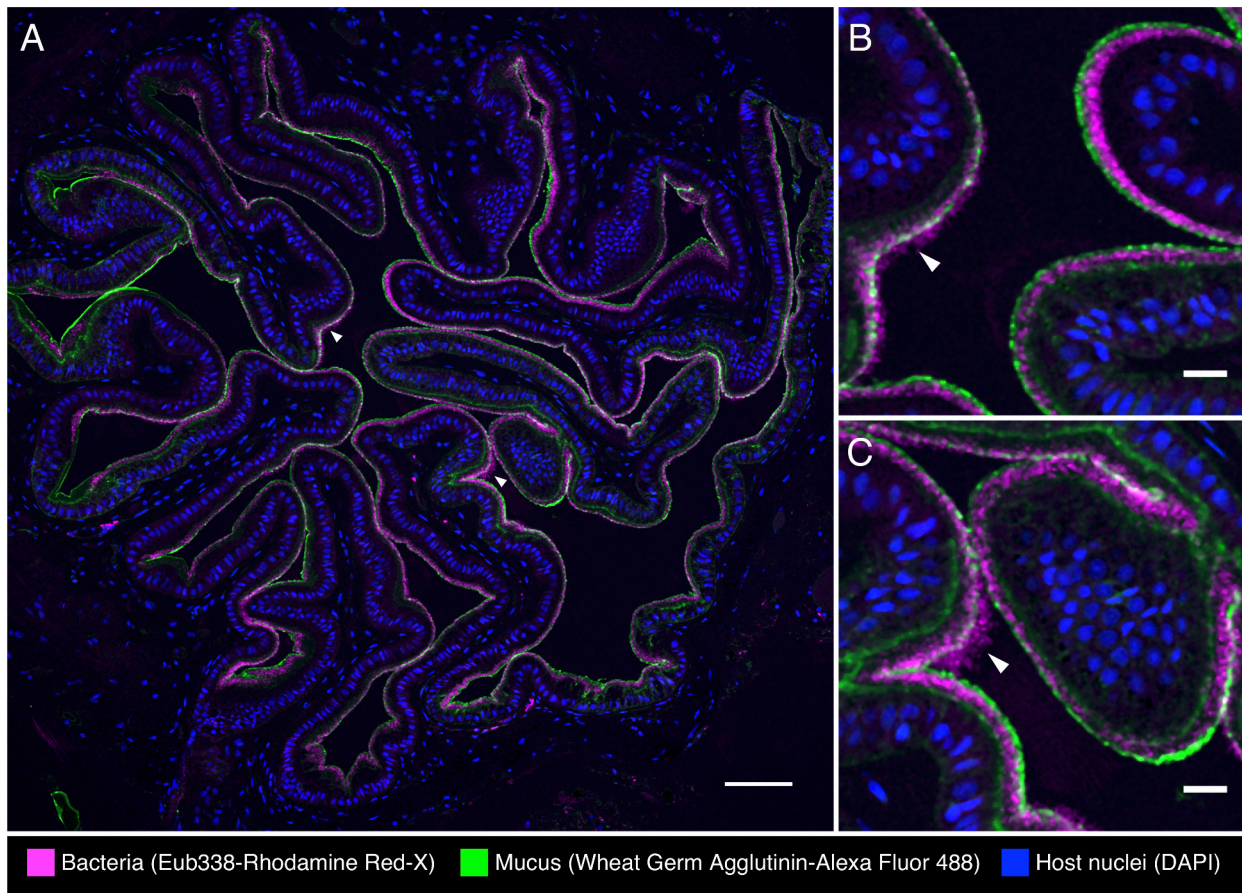
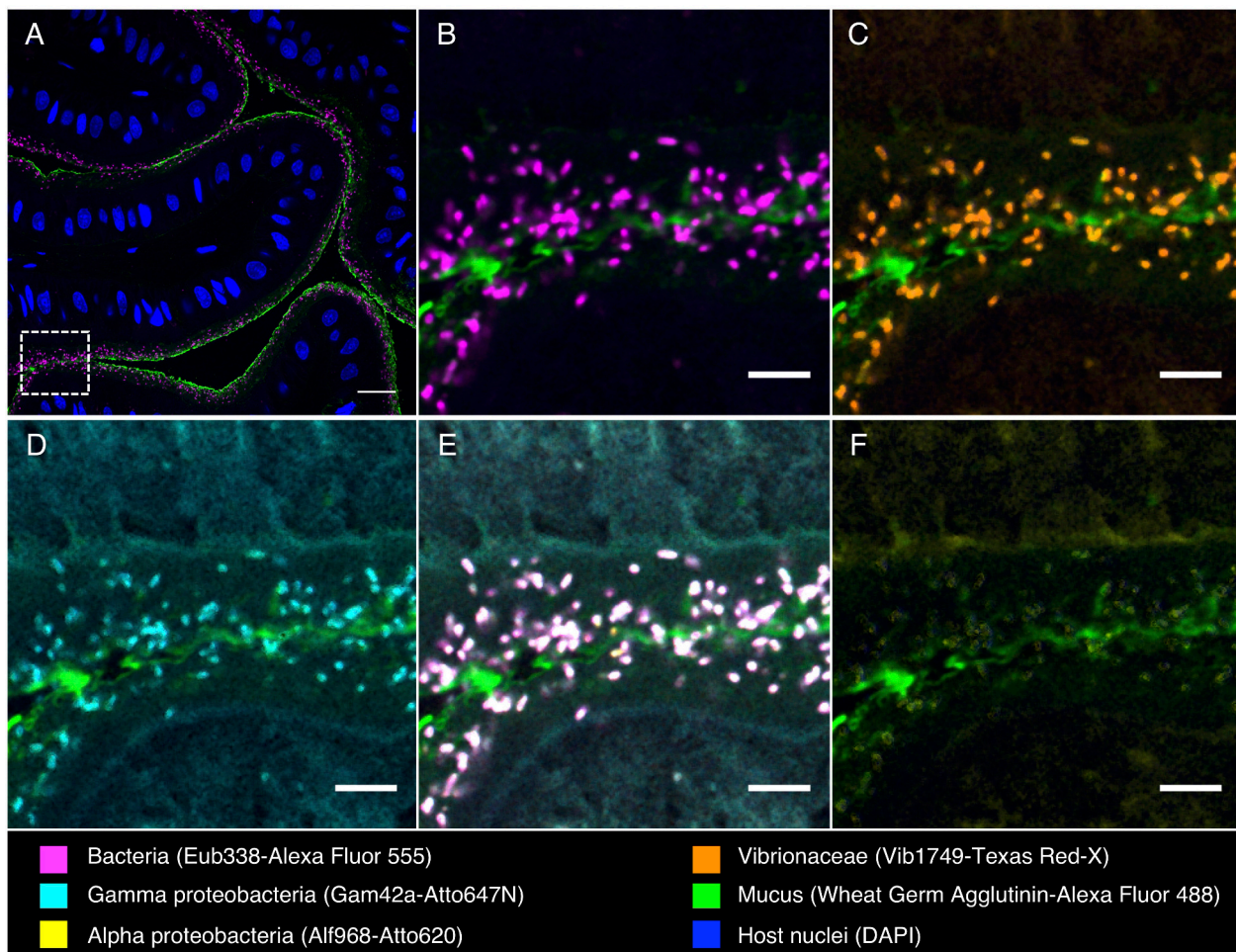


Figure 4. Fluorescence in situ hybridization identifies bacteria in the esophagus of *S. officinalis* as Vibrionaceae.

A methacrylate-embedded section was hybridized with a nested probe set containing probes for most bacteria, Gammaproteobacteria, Alphaproteobacteria, and Vibrionaceae. (A) Near-universal probe showing a similar bacterial distribution as in figure 2. (B - D) Enlarged images of the region marked by the dashed square in (A), showing hybridization with near-universal, Vibrionaceae, and Gammaproteobacteria probes, respectively. (E) Merged image of (B, C, and D) showing an exact match of the signal from those three probes. (F) Alphaproteobacteria probe showing no hybridization. (G) An independent hybridization with the non-target probe set as a control; no signal is observed. (H) enlarged image of the region marked by the dashed square in (G). Scale bar=20 μ m (A, G); 5 μ m (B - F).

Specific probe set



Non-target probe set

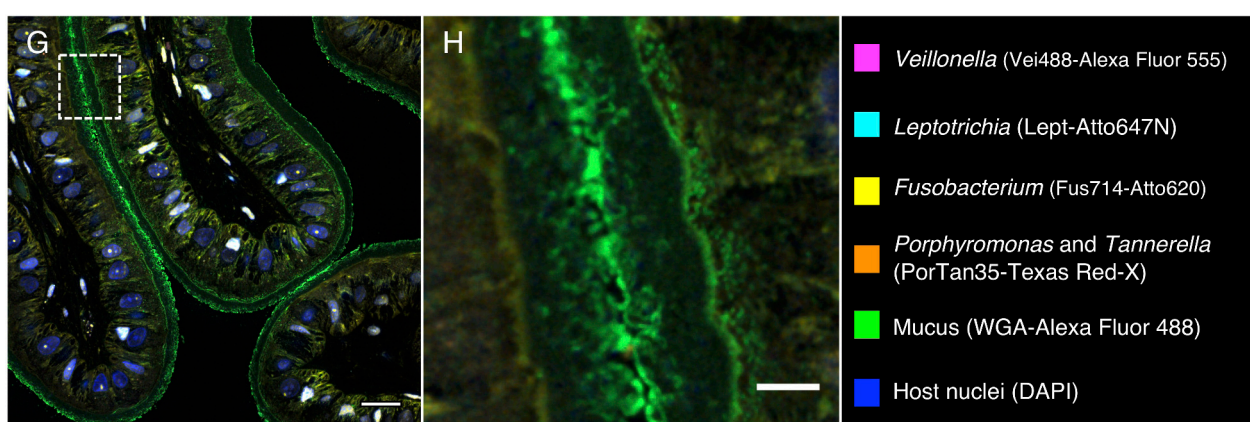


Figure 5. Fluorescence *in situ* hybridization in intestine of *S. officinalis*. A methacrylate-embedded section was hybridized with the near-universal probe and stained with fluorophore-labeled wheat germ agglutinin to visualize mucus (green). (A) Bacteria (magenta) are sparsely distributed through the lumen. (B) enlarged image of the region marked by the dashed square in (A). (C) An independent FISH control with a non-target probe (Hhaem1007); no signal was detected. Scale bar= 20 μ m (A, C); 5 μ m (B).

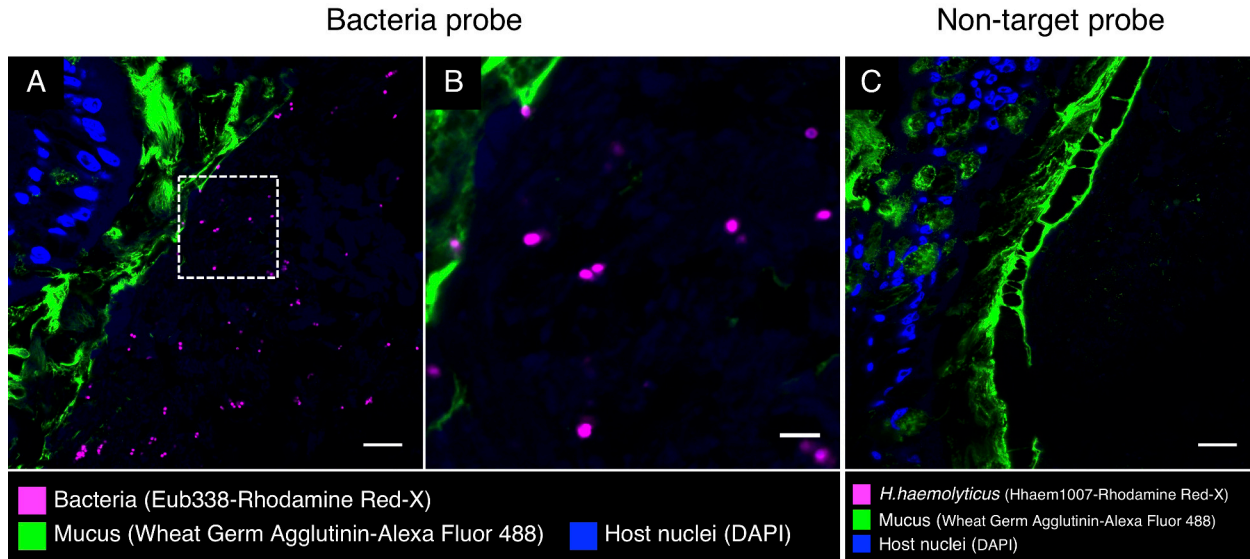


Figure 6. Fluorescence *in situ* hybridization in cecum of *S. officinalis*. A methacrylate-embedded section was hybridized with the near-universal probe and stained with fluorophore-labeled wheat germ agglutinin to visualize mucus (green). (A) Bacteria are observed in low abundance in the lumen of cecum. (B) Enlarged image of region marked by the dashed square in (A). Scale bar=20 μ m (A); 5 μ m (B).

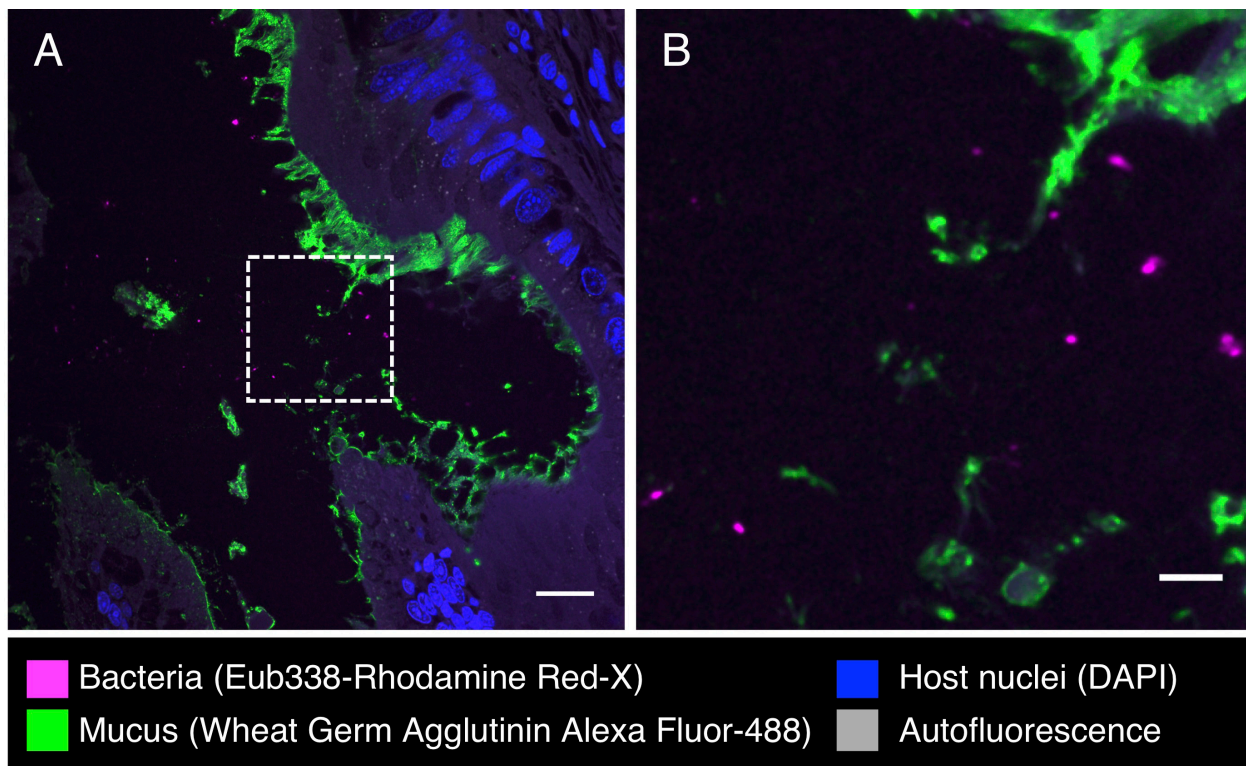


Figure 7. Fluorescence *in situ* hybridization in gills of *S. officinalis*. A methacrylate-embedded section was hybridized with the near-universal probe and stained with fluorophore-labeled wheat germ agglutinin to visualize mucus (green). Bacteria are observed in small clusters. (A) Overview image. (B, C): enlarged images of the region marked by the dashed square in (A) showing hybridization with near-universal, and Gammaproteobacteria probes, respectively. (D) Merged image of (B), and (C) showing an exact match of the signal from those two probes. Display in (B, C, and D) was adjusted for clarity. Scale bar=20 μ m (A); 5 μ m (B-D).

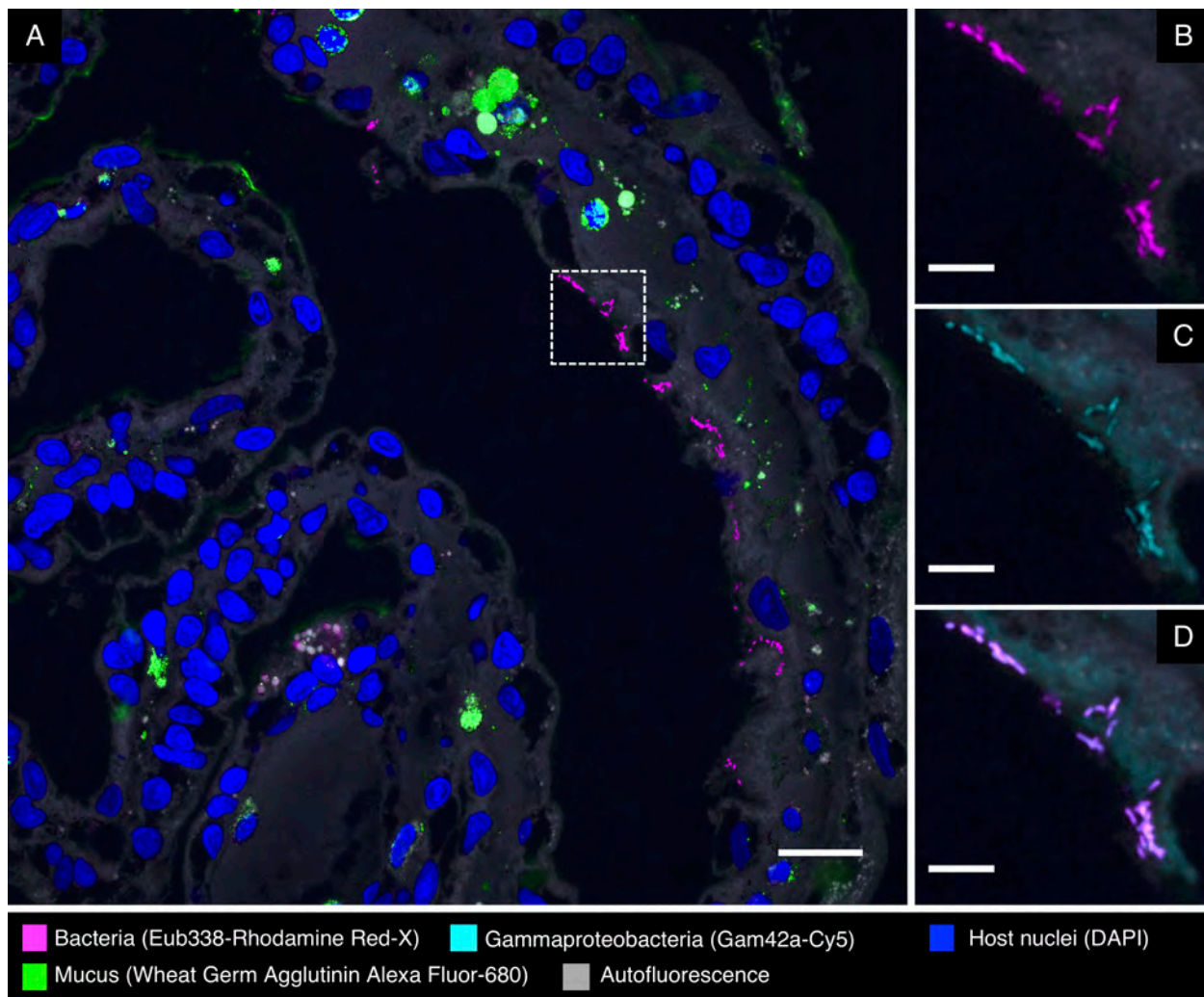


Table 1. Relative abundance of three most abundant ASVs found among two sampling periods of the European common cuttlefish. Averages correspond to relative abundance of individual ASVs from each anatomical site and period. Period 1 consisted of three individuals, Period 2 consisted of eight individuals.

Anatomical Site	ASV1			ASV2			ASV3		
	Pilot	Control	Antibiotic	Pilot	Control	Antibiotic	Pilot	Control	Treatment
Esophagus	0.92 ± 0.10	1.00 ± 0.01	0.94 ± 0.10	0.07 ± 0.10	0 ± 0	0 ± 0	0 ± 0	0 ± 0	0 ± 0
Stomach	0.39 ± 0.34	0.43 ± 0.37	0.19 ± 0.31	0.25 + 0.42	0 ± 0	0 ± 0	0 ± 0	0 ± 0	0 ± 0
Cecum	0.24 ± 0.14	0.44 ± 0.23	0.06 ± 0.09	0.28+0.35	0 ± 0	0 ± 0	0 ± 0	0 ± 0	0 ± 0
Intestine	0.22 ± 0.42	0.57 ± 0.16	0.06 ± 0.06	0.50 ± 0.57	0.01 ± 0.01	0 ± 0	0 ± 0	0 ± 0	0 ± 0
Gills	0 ± 0	0 ± 0	0 ± 0	0 ± 0	0.01 ± 0.01	0 ± 0	0.79 ± 0.11	0.97 ± 0.03	0.82 ± 0.19
Skin	0.02 ± 0.03	0.08 ± 0.11	0.01 ± 0.02	0.03 ± 0.02	0 ± 0	0 ± 0	0 ± 0	0 ± 0	0.01 ± 0.02

1

2

Table 2. FISH probes used in this study

	Probe name	Fluorophore(s)	Target organism	Sequence 5' – 3'	Target position	Reference
Experimental probe set	Eub338-I	Alexa 555 or Rhodamine Red-X	Most Bacteria	GCTGCCTCCGTAGGAGT	16S, 338-355	Amann et al. 1990
	Vib1749	Texas Red-X	Vibrionaceae family	AGCCACCTGGTATCTGCGACT	23S, 1749-1769	Schlundt et al., in prep
	Vib2300	Texas Red-X	Vibrionaceae family	TAACCTCACGATGTCCAACCGTG	23S, 2299-2321	Schlundt et al., in prep
	Alf968	Atto 620 or Dy490	Alphaproteobacteria	GGTAAGGTTCTGCGCGTT	16S, 968-985	Neef, A., 1997
	Gam42a	Atto 647N or Cy5	Gammaproteobacteria	GCCTTCCCACATCGTT	23S, 1027-1043	Manz et al. 1992
Non-target control probe set	Vei488	Alexa 555	<i>Veillonella</i>	CCGTGGCTTCTATTCCG	16S, 488-505	Chalmers et al. 2008
	PorTan34	Texas Red-X	<i>Porphyromonas</i> and <i>Tannerella</i>	GTAAAGCCTATCGCTAGC	16S, 34-51	Mark Welch et al., in prep.
	Fus714	Atto 620	<i>Fusobacterium</i>	GGCTTCCCCATCGGCATT	16S, 714-731	Valm et al. 2011
	Lept568	Atto 647N	<i>Leptotrichia</i>	GCCTAGATGCCCTTTATG	16S, 568-585	Valm et al. 2011
Non-target probe	Hhaem1007	Rhodamine Red-X	<i>Haemophilus haemolyticus</i>	AGGCACTCCCATATCTCTACAG	16S, 1007-1028	Mark Welch et al., in prep.

3

4